Part III

Supernovae: Progenitors/Remnants

https://doi.org/10.1017/S0252921100009209 Published online by Cambridge University Press

Pre-Supernova Evolution of Rotating Massive Stars

Raphael Hirschi[1], Georges Meynet[1], André Maeder[1], and Stéphane Goriely[2]

[1] Observatoire de Genève, 1290 Sauverny, Switzerland;
raphael.hirschi@obs.unige.ch
[2] Université Libre de Bruxelles, Bruxelles, Belgique

Summary. The Geneva evolutionary code has been modified to study the advanced stages (Ne, O, Si burnings) of rotating massive stars. Here we present the results of four 20 $M_\odot$ stars at solar metallicity with initial rotational velocities, $v_{\rm ini}$, of 0, 100, 200 and 300 km/s in order to show the crucial role of rotation in stellar evolution. As already known, rotation increases mass loss and core masses [4]. A fast rotating 20 $M_\odot$ star has the same central evolution as a non-rotating 26 $M_\odot$. Rotation also increases strongly net total metal yields. Furthermore, rotation changes the SN type so that more SNIb are predicted (see [5] and [6]). Finally, SN1987A-like supernovae progenitor colors can be explained in a single rotating star scenario.

1 Computer Model

The computer model used is the Geneva evolutionary code (see [5]). Convective stability is determined by the Schwarzschild criterion. The overshooting parameter, $\alpha_{\rm over} = d_{\rm over}/H_{\rm P}$ is equal to 0.1 for hydrogen- and helium-burning cores and equal to 0 afterwards. Modifications have been made to study the advanced stages of the evolution of rotating massive stars. Dynamical shear has been included using $Ri_c = 1/4$ [2]. Note that the computer model still includes secular shear and meridional circulation. The structure equations have been stabilized using Sugimoto's prescription [7]. Furthermore, convection is treated as diffusion from the Oxygen (O) burning stage because convection is no longer instantaneous. The algorithm developed for rotational mixing is used for this purpose. Finally, the nuclear reaction network has been extended and contains all the multiple-α elements up to ^{56}Ni except ^{8}Be. The reaction rates are taken from the NACRE compilation or Hauser-Feschbach code calculations (ULB, Belgium).

2 Evolution

The early evolutionary stages are presented in [5]. Here we concentrate on solar metallicity 20 $M_\odot$ stars and study the effect of rotation by examining four models with initial rotational velocities of 0, 100, 200 and 300 km/s. Calculations have been followed until end of central O-burning for the $v_{\rm ini}$ =

https://doi.org/10.1017/S0252921100009209 Published online by Cambridge University Press

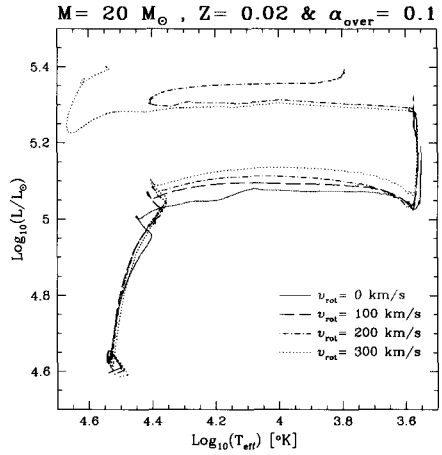

Fig. 1. HR diagram for the solar metallicity $20\,M_\odot$ stars with initial rotational velocities of 0, 100, 200 and 300 km/s.

100 and 200 km/s models, end of central Si-burning for the $v_{\rm ini} = 300$ km/s model and end of first shell Si-burning for the non-rotating model.

2.1 Hertzsprung-Russell (HR) Diagram

Figure 1 shows the evolutionary tracks of the four different $20\,M_\odot$ stars in the HR diagram. The non-rotating model ends up as a red supergiant (RSG) like other group models (see, e.g., [1] or [3]). However, the rotating models show very interesting features. Although the 100 km/s model remains a RSG, the 200 km s^{-1} model undergoes a blue loop to finish as a yellow-red supergiant whereas the 300 km s^{-1} model ends up as a blue supergiant (BSG). Thus rotation may strongly affect the shock wave travel time through the envelope when the star explodes in a supernova event, since this time is proportional to the radius of the star (RSG radii are about hundred times BSG ones). Moreover, the behavior of the models with $v_{\rm ini}$ between 200 and 300 km s^{-1} is reminiscent of the evolution of the progenitor of 1987A indicating that rotation may play a role in similar cases.

2.2 Central Evolution

The central evolution is best seen in the central temperature, T_c, versus central density, ρ_c, diagram (Fig. 2). We can see that rotation makes the cores slightly less degenerate (higher T_c and smaller ρ_c). This is explained by the bigger core masses. We also see that the "C-bump" due to the convective central C-burning fades away when rotation increases (see also Fig. 3). This is again a consequence of more massive cores in rotating models which implies

https://doi.org/10.1017/S0252921100009209 Published online by Cambridge University Press

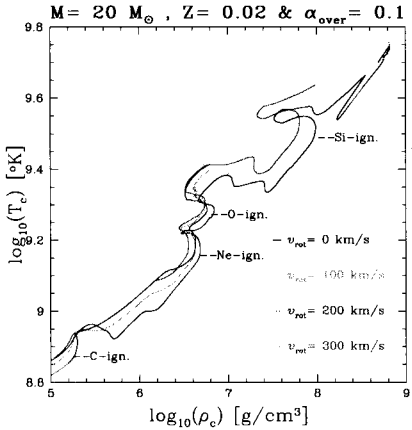

Fig. 2. T_c versus ρ_c diagram.

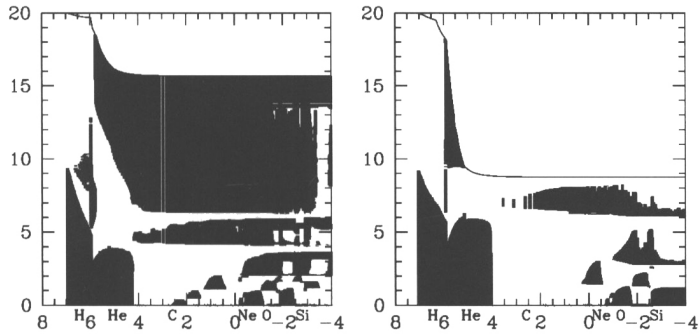

Fig. 3. Kippenhahn diagrams: mass ($M_\odot$) versus $\log_{10}$(∼ time left until core collapse) (yr). *Left* non-rotating $20\,M_\odot$ model. *Right* $\upsilon_{\rm ini} = 300\,$km/s $20\,M_\odot$ model. Colored zones show convective zones. Letters indicate burning stages.

higher neutrino loss rates and smaller central carbon abundance at the end of He-burning phase.

3 "Pre-SN" Models

3.1 Mass Loss and Core Masses

We can see in Fig. 4 that both mass loss and helium (He) core masses, M_α, increase with rotation as already known. There is a saturation effect at high rotation when the star is left with hardly any hydrogen (H) envelope. As can be seen in [5], rotation noticeably increases the number of Wolf-Rayet stars (WR). Here we see that there is a smooth transition between SN type from

https://doi.org/10.1017/S0252921100009209 Published online by Cambridge University Press

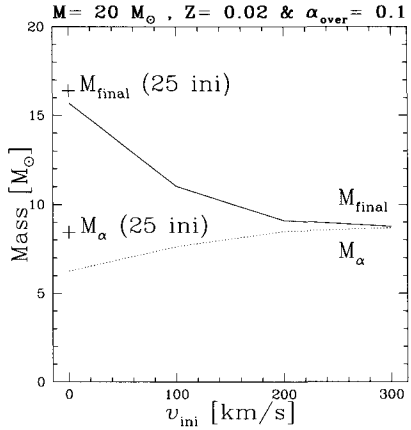

Fig. 4. Final total mass, M_{final}, and helium core mass, M_α, as a function of v_{ini}. Non-rotating 25 $M_\odot$ model masses are also shown for comparison.

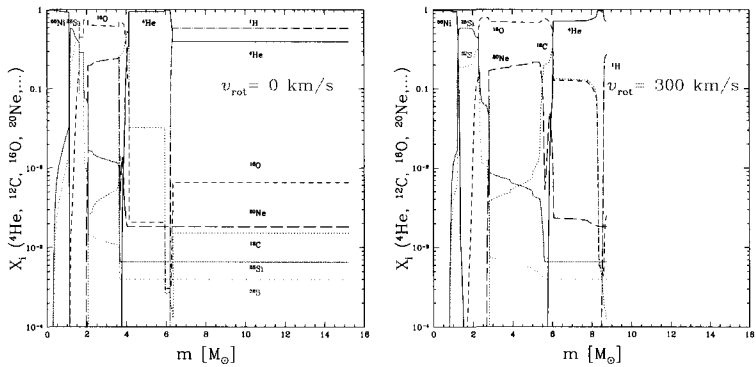

Fig. 5. Abundances profile for main elements at the end of central Si-burning. *Left* non-rotating 20 $M_\odot$ model. *Right* v_{ini} = 300 km/s 20 $M_\odot$ model.

IIP → IIL → IIb (→ Ib). We also note that the v_{ini} = 300 km s^{-1} 20 $M_\odot$ model has a bigger He core than the non-rotating 25 $M_\odot$ model (it would correspond to the core of a non-rotating 26 $M_\odot$ model). The carbon-oxygen core mass, M_{CO}, increases with rotation in a similar way as M_α. The Silicon (Si) core mass at the end of central O-burning only slightly increases with rotation.

3.2 Abundances Profile and Net Yields

In Fig. 5 we notice the smoother profiles due to rotational mixing and also the very small quantity of remaining H. The "pre-SN" net yields calculated at this stage show that rotation increases the total metal yield and ^{16}O yield.

https://doi.org/10.1017/S0252921100009209 Published online by Cambridge University Press

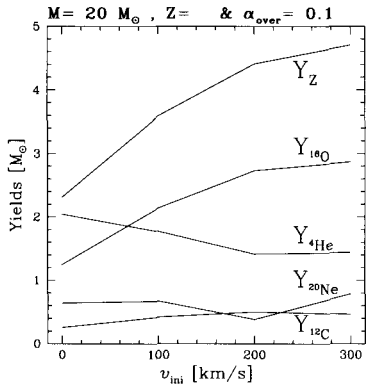

Fig. 6. Net yields of the sum of all metals, Y_Z, and individual elements as a function of $v_{\rm ini}$.

Typically, the total metal yield of the $v_{\rm ini} = 300$ km s^{-1}model is twice the one of the non-rotating model. On the other hand, rotation decreases H-burning products yields (notably ^{4}He) as can be seen in Fig. 6.

References

1. A. Heger, N. Langer: Astrophys. J. **544**, 1016 (2000)
2. R. Hirschi et al. : astro-ph 0301357 (2003)
3. M. Limongi, O. Straniero, A. Chieffi: Astrophys. J. Suppl. **129**, 625 (2000)
4. G. Meynet, A. Maeder: Astron. Astrophys. **361**, 101 (2000)
5. G. Meynet, A. Maeder: Astron. Astrophys. **404**, 975 (2003)
6. N. Prantzos, S. Boissier: Astron. Astrophys. **406**, 259 (2003)
7. D. Sugimoto: Astrophys. J. **159**, 619 (1970)

https://doi.org/10.1017/S0252921100009209 Published online by Cambridge University Press